Parallel Imaging Based on Multicore DSP for FMCW SAR

Chengfei Gu, Wenge Chang, and Xiangyang Li
College of Electronic Science and Engineering
National University of Defense Technology, Changsha, Hunan 410073, China

Abstract— A Ku-band FMCW SAR system is demonstrated which has the capability of real-time processing with the application of single high-performance multi-core DSP. The navigational data of platform movement, which particularly used for high precision motion compensation, is accurately measured by GPS and accelerometer. Furthermore, to realize the real-time processing, the parallel processing approach based on multicore DSP is presented in detail, also the time consumptions of key steps are minutely listed. To verify the capability of real-time processing, several automobile experiments are campaigned with the FMCW SAR sensor on the top of the car. The obtained results of real-time processing and post-processing are presented and compared, processed with 35 cm and 25 cm resolution, respectively.

1. INTRODUCTION

The combination of frequency modulated continuous wave (FMCW) and synthetic aperture radar (SAR) leads to a compact and high-resolution imaging sensor, and this makes FMCW SAR be a hot spot in recent SAR research [1, 2]. FMCW SAR not only has the characteristics of day-or-night and adverse-weather operation, but also holds the advantages of lightweight and low power consumption. Predictably, FMCW SAR will have enormous potential application in remote sensing and mapping. However the main challenge of this compact and high-resolution sensor is the realization of real-time imaging.

Because of the finite board load and rigid time requirement, the real-time processing of FMCW SAR has been a bottleneck. In this paper, only a highly integrated multicore digital signal processor (DSP) is chosen as the processing kernel [3]. It is known that the automobile based SAR experiment is flexible and essential for FMCW SAR system debug before the airborne based experiment [4, 5]. In order to validate the performance of real-time SAR imaging, several automobile experiments have been successfully performed. At the end of this paper, the real-time processing and post-processing imageries are showned and compared, processed with 35 cm and 25 cm resolution, respectively.

The remainder of this paper is briefly organized as follows. In Section 2, the imaging algorithm for FMCW SAR is reviewed. Section 3 depicts the parallel processing flow of real-time imaging, also the time consumptions are minutely listed. In Section 4, the results of real-time processing and post processing are presented and compared, also the qualities of corner reflects are analyzed in detail. Finally, Section 5 gives the conclusion of this paper.

2. IMAGING ALGORITHM FOR FMCW SAR

It is known that, for SAR imaging algorithms, the time-domain algorithm is not suitable for the real-time processing. The frequency-domain algorithm includes Range-Doppler Algorithm (RDA), Range Migration Algorithm (RMA), Chirp-Scaling Algorithm (CSA), Frequency-Scaling Algorithm (FSA), etc. [1, 2]. However RMA is not suitable for real-time processing because of its time-consuming interpolation. CSA can't process the deramped signal of FMCW SAR. RDA can only deal with the narrow swath width and low resolution SAR imaging. Hence, in this paper, the extended FSA [1, 2] is chosen as the real-time processing algorithm. The imaging geometry of automobile experiment is shown in Fig. 1.

The expression of the transmitted FMCW signal is [1, 2]

$$s_t(\hat{t}, t_m) = rect\left(\frac{\hat{t}}{T_p}\right) \cdot \exp\left[j2\pi\left(f_c t + \frac{1}{2}\gamma \hat{t}^2\right)\right] \tag{1}$$

in which $\hat{t}$ is the fast time, T_p is the signal time width. f_c and γ are the carrier frequency and the chirp rate of transmitted signal, respectively. The deramped signal is simplified as [1,2]

$$s_{if}(\hat{t}, t_m) = A \cdot rect\left(\frac{\hat{t} - 2R'/c}{T_p}\right) \cdot \exp\left[-j\frac{4\pi}{\lambda}R_B\right] \cdot \exp\left[-j\frac{4\pi\gamma\hat{t}}{c}R'\right] \cdot \exp\left(-j2\pi f_d \hat{t}\right) \cdot \exp\left[j4\pi\gamma\left(\frac{R'}{c}\right)^2\right] \tag{2}$$

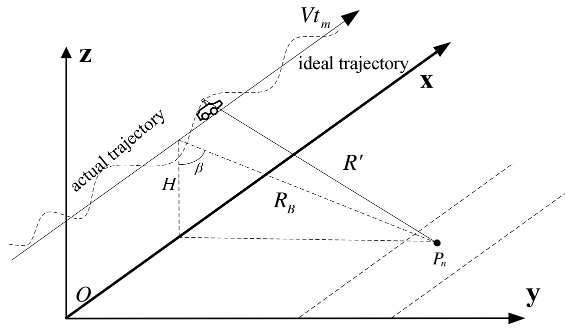

Figure 1: Automobile based imaging geometry.

where the variable R' and R_B are the instantaneous range and the zero-doppler slant range from sensor to point P_n. t_m is the slow time, $f_d$is the doppler frequency in azimuth. c and λ stand for the light velocity and the wavelength, respectively. The first exponential term and the second one represent the doppler modulation in azimuth and the signal in range. The third exponential term is the range migration introduced by the platform movement within a sweep. The last one is the residual video phase (RVP), and the frequency scaling algorithm is based on the RVP term [1, 2].

3. REAL-TIME PROCESSING FLOW

3.1. Signal Processing Flow

The data flow of real-time processing is shown in Fig. 2.

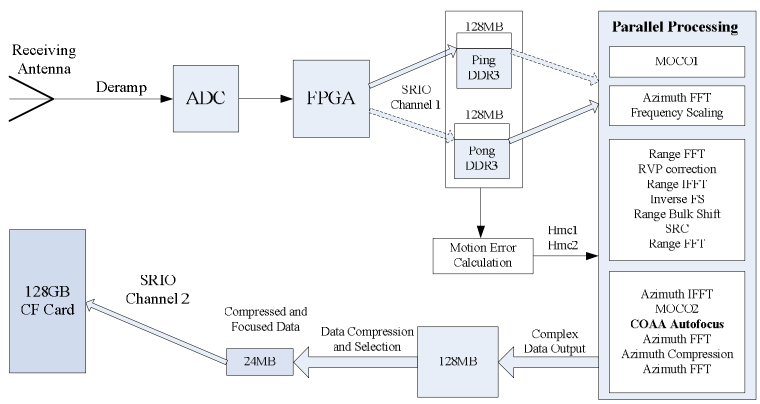

Figure 2: Data flow of real-time processing.

As shown in Fig. 2, the received signal is digitally recorded after the ADC. And FPGA buffers the raw data into DDR3 SDRAM through the SRIO channel 1. The motion error of Ping or Pong data matrix is accurately measured based the GPS and accelerometer data. After the motion error calculation, the data matrix is under parallel processing by multicore DSP [6]. The parallel processing contains basic FS processing, two-order motion compensation and COAA autofocus. The output of the parallel processing is the complex float data with a size of 128MB. The following process is data compression and selection. After the compression and selection of processed data, the focused imaging data is stored into CF card using the SRIO channel 2.

3.2. Automobile Experiment and the Time-consuming

The proposed parallel imaging flow has been validated on a compact FMCW SAR sensor, which carries an eight-core DSP. The compact FMCW SAR sensor is mounted on the top of a sport utility vehicle (SUV), and the recorded raw data undergo real-time processing onboard. The signal bandwidth is 600 MHz, and the velocity of SUV is about 16.2 m/s. The swath width and the center slant range are 800 m and 1 km, respectively. The time consumptions of real-time processing are listed in Table 1.

As listed in Table 1, the motion error calculation of data matrix is about 0.0168 s. The parallel processing time of FS algorithm is 1.405 s and the COAA autofocus costs 0.7739 s. Considering

Table 1: Summarizes of real-time processing time-consuming.

Operations	Value (s)
Motion Error Calculation	0.0168
Parallel FS Processing	1.4050
Parallel COAA Autofocus	0.7739
Data Compression	0.0684
Overlapped Data Transmission	0.0119
Focused Data Storage	0.3030
Total Processing Time	**2.579**

the throughput of CF card, the storage time of focused data is about 0.303 s. The total time consumption of the parallel processing flow is about 2.579 s, which satisfies 3.072 s real-time limit.

4. RESULTS AND QUALITY ANALYSIS

4.1. Images of Real-time and Post Processing

After times of automobile experiments, some beneficial real-time processing results are gained. Fig. 3 shows one of these real-time processed images.

In Fig. 3, the imagery covers areas of 350 m × 400 m (azimuth × range) island and the central slant range is about 1 km. Target 2 is a stone arch bridge and the target 1 is a waterside terrace close to the Xiangjiang River. The optical photographs in Fig. 3 are two targets on the island. Comparing the imaging result with the optical photograph, we can say that the real-time processing result gains well geologic matching. Moreover, the characteristic targets, such as the waterside terrace and the stone arch bridge, are well focused. The real-time processing and post-processing results of the same scene are shown in Fig. 4.

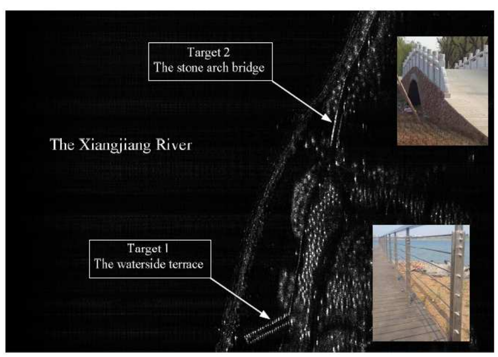

Figure 3: The automobile real-time imaging result.

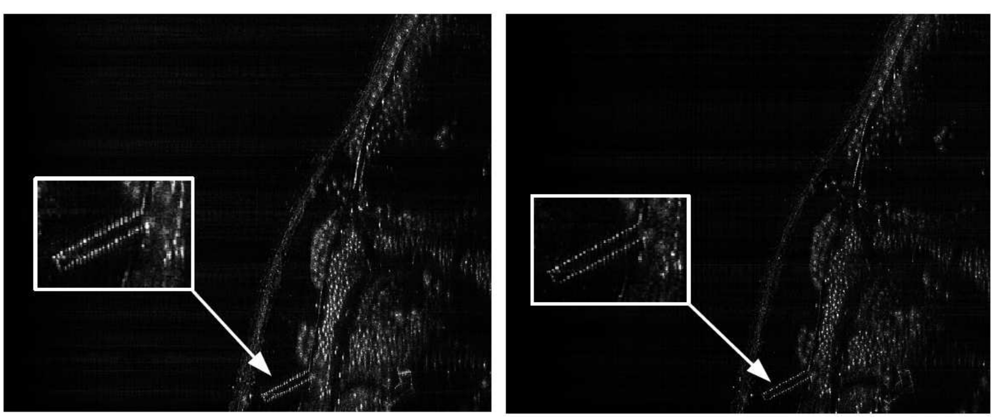

(a) (b)

Figure 4: Comparison of (a) real-time processed and (b) post-processed images.

In Fig. 4, the sub-image (a) is the real-time processed result, and the sub-image (b) is the result of post processing. Comparing Fig. 4(a) with Fig. 4(b), the overall effect of two images are close to each other, and the result verifies the efficiency of the real-time processing flow. Besides the two-order motion compensation and COAA autofocus, the post-processing has also implied the PGA processing. Hence, the focused result of post-processing is better than the real-time one. The analysis result shows that the resolution of post-processed image is about 25 cm.

Table 2: Point targets analysis.

Parameters		$T1$	$T2$	$T3$	$T4$
Range	IRW(m)	0.364	0.334	0.322	0.388
	PSLR(dB)	−25.19	−26.72	−31.38	−25.58
	ISLR(dB)	−16.13	−15.55	−16.21	−14.74
Azimuth	IRW(m)	0.341	0.361	0.352	0.364
	PSLR(dB)	−29.31	−36.17	−31.34	−25.73
	ISLR(dB)	−16.06	−18.67	−15.44	−13.39

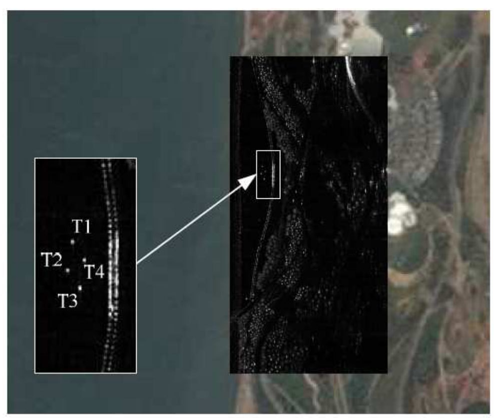

Figure 5: Real-time processing result with corner reflectors.

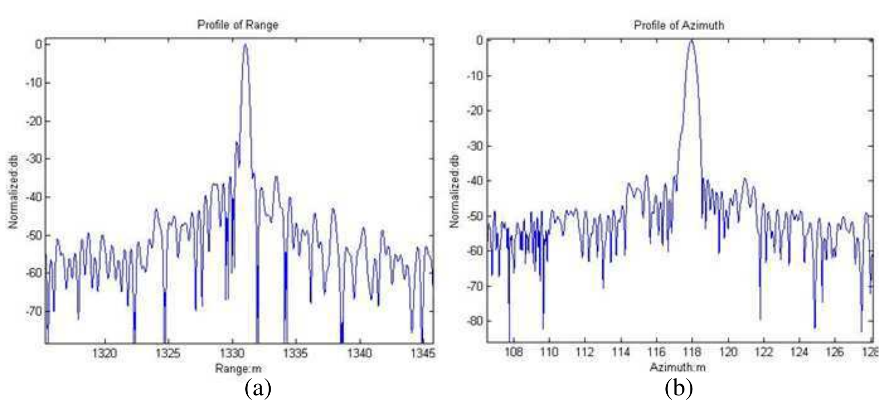

Figure 6: Profiles of $T1$ in (a) range and (b) azimuth.

4.2. Quality Analysis

To assess the quality of real-time processed image, four corner reflectors are specifically scattered on the test field. The real-time imagery with corner reflectors is shown in Fig. 5.

As shown in Fig. 5, the imaging scene is an island with size of 800 m × 350 m (azimuth × range) in the Xiangjiang River with about 1 km central slant range. Targets 1 to 4 in Fig. 5 are four corner reflectors to be analyzed. Two dimensional impulse response width (IRW), peak-to-side lobe ratios (PSLR) of four corner reflectors are listed in Table 2.

The azimuth and range profiles of $T1$ in Fig. 5 are shown in Fig. 6(a) and Fig. 6(b), respectively.

With the application of hamming window, the obtained mean range resolution is about 0.35 cm. Also the average result in azimuth shows a good resolution of 0.35 cm. The PSLR and ISLR results are both good. In a word, the analysis results demonstrate a high focusing quality. The efficiency of proposed real-time processing flow is also validated.

5. CONCLUSION

A compact real-time processing SAR sensor is presented in this paper. On the foundation of this compact SAR system, the FSA which also contains two-order motion compensation and time-consuming COAA autofocus processing is efficiently realized in parallel with a single eight-core DSP. Furthermore, both the real-time processing result and the post-processing result of automobile experiment are presented and compared, also the quality of SAR images are analyzed in detail.

REFERENCES

1. Meta, A., P. Hoogeboom, and L. P. Ligthart, "Signal processing for FMCW SAR," *IEEE Trans. Geosci. Remote Sens.*, Vol. 45, No. 11, 3519–3532, 2007.
2. Jia, G. W., M. Buchroithner, W. G. Chang, and X. Y. Li, "Simplified real-time imaging flow for high-resolution FMCW SAR," *IEEE Geosci. Remote Sens. Lett.*, Vol. 12, No. 5, 973–977, 2015.
3. "TMS320C6678 multicore fixed and floating-point digital signal processor data manual," Texas Instruments Incorporated, Texas, United States, 2011.
4. Wang, R., Y. H. Luo, Y. K. Deng, and Z. M. Zhang, "Motion compensation for high-resolution automobile FMCW SAR," *IEEE Geosci. Remote Sens. Lett.*, Vol. 10, No. 5, 1157–1161, 2013.
5. Cho, B. L., Y. K. Kong, H. G. Park, and Y. S. Kim, "Automobile-based SAR/InSAR system for ground experiments," *IEEE Geosci. Remote Sens. Lett.*, Vol. 3, No. 3, 401–405, 2006.
6. Gu, C. F., X. Y. Li, W. G. Chang, G. W. Jia, and H. S. Tian, "Matrix transposition based on TMS320C6678," *Proceedings of GSMM*, 29–32, Harbin, China, May 2012.